Applied Petrochemical Research (2018) 8:263–270
https://doi.org/10.1007/s13203-018-0218-5

ORIGINAL ARTICLE

Dry reforming of methane for syngas production over Ni–Co-supported Al_2O_3–MgO catalysts

Nur Azeanni Abd Ghani[1] · Abbas Azapour[2] · Syed Anuar Faua'ad Syed Muhammad[3] · Nasser Mohamed Ramli[4] · Dai-Viet N. Vo[5,6] · Bawadi Abdullah[1,4]

Received: 22 May 2018 / Accepted: 8 November 2018 / Published online: 21 November 2018

Abstract

This research project focuses on the development of catalysts for syngas production by synthesizing Ni–Co bimetallic catalyst using aluminum oxide (Al_2O_3) and magnesium oxide (MgO) as the catalyst support. Ni/Al_2O_3 (CAT-1), Ni–Co/Al_2O_3 (CAT-2) and Ni–Co/Al_2O_3–MgO (CAT-3) nanocatalysts were synthesized by sol–gel method with citric acid as the gelling agent, and used in the dry reforming of methane (DRM). The objective of this study is to investigate the effects of Al_2O_3 and MgO addition on the catalytic properties and the reaction performance of synthesized catalysts in the DRM reactions. The characteristics of the catalyst are studied using field emission scanning electron microscope (FESEM), Brunauer–Emmett–Teller (BET), X-ray powder diffraction (XRD), transmission electron microscopy, H_2-temperature programmed reduction, CO_2-temperature programmed desorption and temperature programmed oxidation analysis. The characteristics of the catalyst are dependent on the type of support, which influences the catalytic performances. FESEM analysis showed that CAT-3 has irregular shape morphology, and is well dispersed onto the catalyst support. BET results demonstrate high surface area of the synthesized catalyst due to high calcination temperature during catalysts preparation. Moreover, the formation of $MgAl_2O_4$ spinel-type solution in CAT-3 is proved by XRD analysis due to the interaction between alumina lattice and magnesium metal which has high resistance to coke formation, leading to stronger metal surface interaction within the catalyst. The CO_2 methane dry reforming is executed in the tubular furnace reactor at 1073.15 K, 1 atm and CH_4/CO_2 ratio of unity to investigate the effect of the mentioned catalysts. Ni–Co/Al_2O_3–MgO gave the highest catalyst performance compared to the other synthesized catalysts owning to the strong metal–support interaction, high stability and significant resistance to carbon deposition during the DRM reaction.

Keywords Catalyst development · Dry reforming · Bimetallic catalysts · Catalysis · Sol–gel · Support

Introduction

Recently, the global warming issue is getting crucial due to the substantial dependence on petroleum-based energy that leads to the increment of greenhouse-gas emissions within the atmosphere [30]. The concentration of CO_2 in the atmosphere has currently increased by about 1.5 ppm/year which indicated that if there is about 5.3×10^{21} g air, the rate of CO_2 increase is about 8 billion tons per year [5]. These realities encouraged the study on the development

✉ Bawadi Abdullah
bawadi_abdullah@utp.edu.my; bawadi73@gmail.com

[1] CO2 Utilization Group, Institute of Contaminant Management for Oil and Gas, Universiti Teknologi PETRONAS, Bandar Seri Iskandar, 32610 Perak, Malaysia

[2] Faculty of Engineering and Applied Science, Memorial University, St. John's, NL A1B 3X5, Canada

[3] Bioprocess and Polymer Engineering Department, Faculty of Chemical and Energy Engineering, Universiti Teknologi Malaysia, Skudai, 81310 UTM Johor, Malaysia

[4] Chemical Engineering Department, Universiti Teknologi PETRONAS, Bandar Seri Iskandar, 32610 Perak, Malaysia

[5] Faculty of Chemical and Natural Resources Engineering, Universiti Malaysia Pahang, Lebuh Raya Tun Razak, Gambang, Kuantan, 26300 Pahang, Malaysia

[6] Centre of Excellence for Advanced Research in Fluid Flow, Universiti Malaysia Pahang, Lebuh Raya Tun Razak, Gambang, Kuantan, 26300 Pahang, Malaysia

of CO_2 reforming of methane that would effectively reduce the level of CO_2 and CH_4 within the atmosphere.

Steam reforming of methane (SRM), partial oxidation of methane (POM) and methane dry reforming (DRM) [7] are three common techniques which have been used in industries. SRM is used conventionally for hydrogen generation [17, 35]. However, a foreseeable drawback of this process is the production of H_2/CO with the ratio of 3:1 that is undesirable for Fischer–Tropsch (F–T) synthesis. CO_2 reformation of methane is based on the utilization of CO_2 and CH_4 to convert these gases into syngas with low or adjustable hydrogen–carbon monoxide ratio (H_2/CO), which is a desirable feedstock for F–T synthesis to gain liquid hydrocarbons [9, 10, 13]. Therefore, DRM has been considered as the favorable process for syngas production compared to steam reforming and partial oxidation, since it produces lower H_2/CO ratio that is appropriate for downstream F–T synthesis [13]. Yet, the industrial applications of DRM are still facing vast challenges in terms of process engineering and catalysts stability [20]. DRM involves high operating temperatures, usually between 900 and 1273 K to enhance the conversions, and low operating pressures to favor the forward reaction in DRM [6]. The DRM reaction is shown in Eq. (1):

$$CO_2(g) + CH_4(g) \rightarrow 2CO(g) + 2H_2(g) \quad \Delta H = 257\,\text{kJ/mol}. \tag{1}$$

Ni-based catalysts are the best alternatives for the noble metals to be used in the DRM reaction as they have high catalytic performances, wide availability and low cost [11, 24]. Eventhough Ni/Al_2O_3 catalyst has been utilized broadly as DRM reaction catalyst, it encounters a rapid catalyst deactivation that restricts its industrial application. Coke formation [9, 26, 28] and sintering of catalyst at high temperature [17, 35] are the main reasons of the catalyst deactivation. The coke formation primarily originates from two side reactions in DRM which are methane cracking reaction (Eq. 2) and Boudouard reaction (Eq. 3). Also, the highly endothermic nature of DRM reaction requires high temperatures to achieve the desirable conversions [6]. Thus, most of the catalysts are not thermally stable at these conditions due to the sintering of catalyst or collapse of the crystal structure [22]. Hence, it is important to develop a novel catalyst which meets these significant criteria such as high thermal stability of the support, better resistance to coke formation, and sintering of the active phase and high activity throughout the reaction time to achieve the equilibrium conversions [22]:

$$CH_4(g) \rightarrow C + 2H_2(g), \tag{2}$$

$$2CO(g) \rightarrow C + CO_2(g). \tag{3}$$

The development of cost-effective catalysts having higher catalytic activity and more considerable resistance to carbon formation is one of the most concerning issues to commercialize DRM reaction in the industries [3]. One of the approaches applied for the DRM reaction to develop high carbon resistance of Ni-based catalyst is the addition of second metal [8]. The addition of a non-noble metal such as cobalt is more preferable from the economic point of view [8]. Xu et al. [32] proved that the ratio of Ni/Co is closely allied to the catalytic activity of the bimetallic Ni/Co catalysts supported with the γ-Al_2O_3 and doped with La_2O_3. The catalyst having the Ni/Co ratio of 7/3 shows the greatest CH_4 and CO_2 conversion. If the amount of cobalt increases, the catalytic activity decreases. Bimetallic catalyst having ratio of 5/5 and 3/7 exhibits lower catalytic activity than monometallic Ni catalyst [32].

Conventionally, Al_2O_3 is the most proper support for most of the catalytic materials owning to mechanical strength, stability at high temperature and also good textural properties [31]. Although it has been commercially used, the coke deposition is one of the drawbacks of using Al_2O_3 due to its acidic properties. MgO and CeO_2, which are known as the alkaline and alkaline earth oxides, are being used as modifiers of Ni-based catalysts [18] to enhance the metallic dispersion, improve the metal–support interaction, reduce sintering and improve the thermal stability [23, 27]. The basicity of the catalyst is predicted to be increased by the incorporation of MgO and CeO_2. The catalyst basicity improves the adsorption of CO_2 which prevents the formation of coke on the catalyst surface [14, 29, 33].

In present work, the influence of bimetallic Ni–Co catalysts supported with Al_2O_3 and Al_2O_3–MgO in DRM reaction, synthesized by the sol–gel method, is being studied. The synthesized catalysts were characterized and analyzed in tubular furnace reactor to explain the effect of supports on reaction performances to enhance the reactant conversions as well as to minimize the coke formation in DRM reaction.

Experimental section

Materials

The materials used for the catalysts preparation were $Ni(NO_3)_2{\cdot}6H_2O$ (EMSURE ACS, 99%) and $Co(NO_3)_2{\cdot}6H_2O$ (HmbG Chemicals, 97%) as the active metals; $Al(NO_3)_3{\cdot}9H_2O$ (HmbG Chemicals, 98.5%) and $Mg(NO_3)_2{\cdot}6H_2O$ (EMSURE ACS, 99%) as the catalyst supports; and citric acid as the gelling agent. High-purity CO_2, CH_4, N_2 and H_2 (Linde) were used as the laboratory gases for the reaction.

Catalysts preparation

The new Ni–Co bimetallic catalysts were synthesized by direct sol–gel method [19] as it has high potential in producing high homogeneity composition, and improves the particle size distribution in nanoscale levels that could lead to the high catalytic performance [1, 16]. The $Ni(NO_3)_2{\cdot}6H_2O$, $Co(NO_3)_2{\cdot}6H_2O$, $Al(NO_3)_3{\cdot}9H_2O$, $Mg(NO_3)_2{\cdot}6H_2O$, and citric acid were dissolved in deionized water. The continuously stirred mixture was heated using hot plate at 333.15 K until the gel was formed. Consequently, the resulting gel was dried in an oven at 383.15 K overnight, and then calcined in the furnace at 1173.15 K for 5 h. The other samples were also been prepared by the above procedure.

Table 1 includes the formation of the catalysts, including their tagging, molecular structure, description and composition.

Catalyst characterization

FESEM was employed to determine the morphological change by scanning the catalyst samples with a high-energy beam of electrons using a Zeiss Supra_55 VP. Brunauer–Emmett–Teller (BET) analysis was used to determine the specific surface area of a sample—including the pore size distribution. 0.5 g catalyst was used for each analysis using a Micromeritics ASAP 2020. The degassing temperature was set at 383 K to remove the moisture and other adsorbed gases from the catalyst surface.

Furthermore, the phase compositions of the synthesized catalysts were defined by X-ray powder diffraction (XRD) analysis using a Bruker D8B advanced X-ray diffractometer which were recorded in the range $2\theta = 20°–80°$. The crystallite size, t, was estimated from X-ray line broadening using the Scherrer's formula, $t = 0.9{\cdot}\lambda/(B\cos(\theta))$, where λ is the X-ray wavelength (Cu Kα radiation 0.154 nm) and B the full-width half-maximum of the Bragg diffraction angle θ. To study the metal dispersion on the catalyst support, transmission electron microscopy (TEM) was conducted using a HITACHI instrument which operated at 120.0 kV.

Moreover, the reducibility performance of the synthesized catalysts was determined by H_2-temperature programmed reduction (H_2-TPR) analysis technique on a Thermo Finnigan (TPDRO 1100) instrument equipped with a thermal conductivity detector (TCD) in two-stage processes, which are pretreatment and analysis. CO_2-temperature programmed desorption (CO_2-TPD) was used to study the basic properties of the synthesized catalysts. The result is gained from the TP-5000 equipment coupled with a Hiden QIC-20 mass spectrometer. For post-reaction analysis, TPO was used with the same equipment and procedures of H_2-TPR. 0.2 g of the spent catalysts and 5% of O_2/He gas mixture were introduced for the TPO analysis.

Catalytic performance evaluation and testing

The performance of Ni-based supported catalysts in the DRM was studied in a tubular furnace reactor under atmospheric pressure. 0.2 g of the catalyst was held in the middle of the reactor tube between two layers of quartz wool, and the reactor was electrically heated in a furnace. The reactor was purged with N_2 gas at 100 mL min^{-1} to provide an inert atmosphere in the reactor prior to starting the experiment. The reduction process was then carried out at a H_2 flow rate of 20 mL min^{-1} and at a temperature of 1023.15 K for 1 h to activate the catalyst. Then, nitrogen gas was purged again in the reactor until the gas chromatography system showed a complete disappearance of hydrogen gas before the reaction initiation. Methane gas and carbon dioxide with a flow rate of 20 mL min^{-1} for each gas were introduced to the reactor for every run. The reaction took 8 h for every run, and the sample was taken every hour. The effluent from the reactor then was analyzed by an online gas chromatograph (Agilent 7890) with a thermal conductivity reactor (TCD) and a flame ionization detector (FID).

Results and discussion

Morphology

Figure 1 shows the FESEM images of the synthesized catalysts after calcination. CAT-1 and CAT-2 reveal similar morphologies which are the long-shaped nanoparticles. CAT-3 which is Ni–Co/Al_2O_3–MgO shows a clear irregular-shaped morphology image which has a better dispersion onto the catalyst support compared to CAT-2 with a broad size distribution ranging from 20 to 80 nm. The addition of MgO support improves the metal particles dispersion. This leads

Table 1 Mass composition for synthesized catalysts

Catalyst tagging	Catalyst	Description of catalyst	Composition of catalyst
CAT-1	Ni/Al_2O_3	Support: Al_2O_3	15% Ni, 85% Al_2O_3
CAT-2	Ni–Co/Al_2O_3	Support: Al_2O_3	10.5% Ni, 4.5% Co, 85% Al_2O_3
CAT-3	Ni–Co/Al_2O_3–MgO	Support: Al_2O_3 and MgO	10.5% Ni, 4.5% Co, 63.75% Al_2O_3, 21.25% MgO

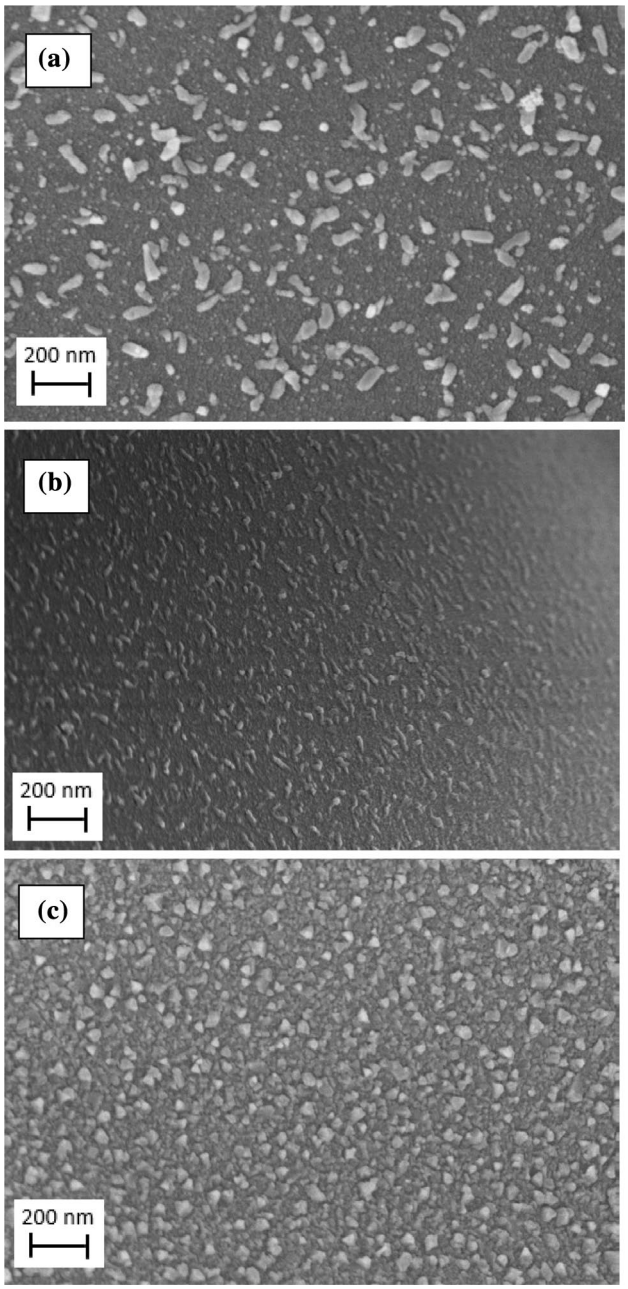

Fig. 1 FESEM images of catalysts at 30.0Kx magnification. **a** CAT-1; **b** CAT-2; **c** CAT-3

to more active sites available for the reaction, and enhances the catalytic performance.

TEM analysis

Figure 2 indicates the TEM analysis results for the synthesized catalysts. Due to the large particles formation, CAT-1 and CAT-2 show a clear catalyst agglomeration. Moreover,

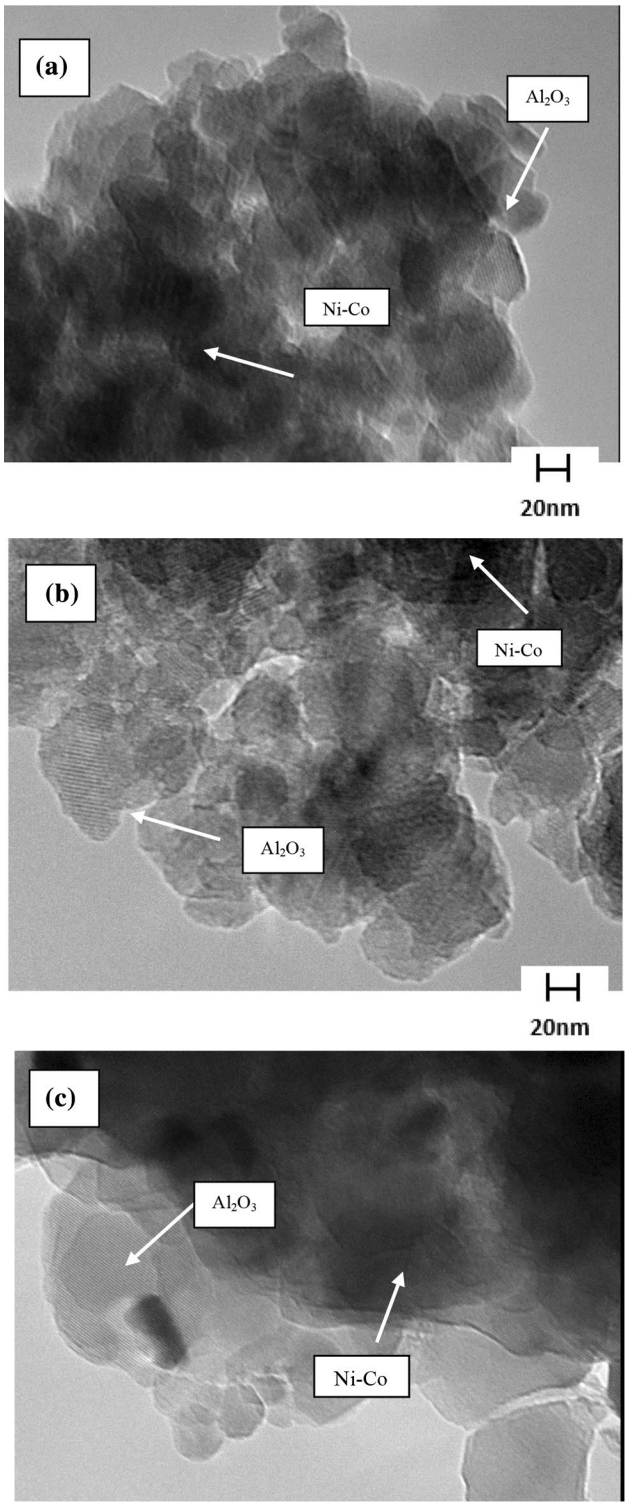

Fig. 2 TEM micrographs of the synthesized catalysts. **a** CAT-1; **b** CAT-2; **c** CAT-3

the TEM micrographs for CAT-3 demonstrates that there are more uniform NiO particles distribution on the catalyst surface that supports the previous FESEM result (cf. Figure 1).

Textural properties

The textural properties of the synthesized catalysts are summarized in Table 2. The surface area and the pore volume for CAT-1, which is Ni–Co/Al_2O_3, were found to be 21.58 $m^2\ g^{-1}$ and 0.04 $cm^3\ g^{-1}$, respectively. Moreover, the surface area and pore volume for CAT-3, which is Ni–Co/Al_2O_3–MgO, were measured to be 9.76 $m^2\ g^{-1}$ and 0.02 $cm^3\ g^{-1}$, respectively. Al-Fatesh and Fakeeha [4] studied on the effect of calcination temperatures on DRM catalysts using Ni/Al_2O_3 and claimed that the high calcination temperature reduces the surface areas but has the advantage of getting the existence of a stable structure of the catalysts. This claim is supported with the BET results in which the catalysts have been calcined at high temperature (1173.15 K).

XRD analysis

Figure 3 illustrates the XRD patterns of the synthesized catalysts at $2\theta = 20°–80°$. The XRD results indicate five crystalline phases formation of $MgAl_2O_4$, Co_3O_4, NiO, MgO and γ-Al_2O_3. The $MgAl_2O_4$ peaks in the form of cubic phase are recognized at 31.6°, 37.3°, 45.3°, 60.0° and 66.2° (JCPDS 00-001-1157) for CAT-3, while Co_3O_4 diffraction peaks are identified at $2\theta = 31.3°$, 36.9°, 44.9°, 59.5°, and 65.3° (JCPDS 01-076-1802) for CAT-2 and CAT-3. The peaks for NiO from $MgAl_2O_4$ and MgO peaks, and peaks for Co_3O_4 from $MgAl_2O_4$ peaks are difficult to differentiate due to the existing overlaps. The figure signifies the patterns existence of NiO peaks at 37.3°, 43.4°, 63.0°, 75.6°, and 79.6° (JCPDS 01-073-1519). For MgO, the diffraction peaks are revealed at $2\theta = 37.0°$, 43.0°, 62.4°, 74.8°, and 78.7° (JCPDS 01-077-2364). The MgO diffraction peaks indicate the high degree of crystallinity in Al_2O_3–MgO support for CAT-3. Furthermore, γ-Al_2O_3 peaks are identified in Ni/Al_2O_3 catalyst at $2\theta = 42.8°$ and 67.3° (JCPDS 00-004-0880) in cubic phase. This analysis indicates that there is an interaction between alumina lattice and magnesium metal to form $MgAl_2O_4$ spinel-type solid solution. $MgAl_2O_4$ has high resistance to carbon formation, and can enhance the metal surface interaction strength [2]. The crystallite sizes calculated using Scherrer's equation are 18.34 nm, 13.1 nm, and 10.73 nm for CAT-1, CAT-2 and CAT-3, respectively. From these observations, it can be concluded that CAT-3 has a better dispersion compared to the other synthesized catalysts, which is supported by the FESEM results (cf. Fig. 1).

Table 2 Textural properties for synthesized catalysts

Catalyst	BET_S (m^2/g)	Pore volume (cm^3/g)	Pore size (Å)
CAT-1	25.57	0.03	48.32
CAT-2	21.58	0.04	57.81
CAT-3	9.76	0.02	107.87

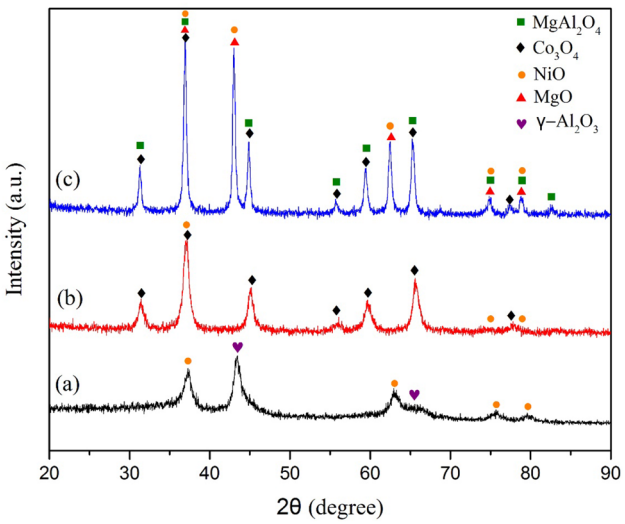

Fig. 3 X-ray diffraction patterns of the catalysts prepared by sol–gel method. (a) CAT-1; (b) CAT-2; (c) CAT-3

H_2-TPR analysis

Figure 4 displays the H_2-TPR analysis for all synthesized catalysts. The TPR patterns are observed to be similar for all synthesized catalysts which have only one peak. The peaks for CAT-1, CAT-2, and CAT-3 are observed at 1180.15 K, 1040.15 K, and 1170.15 K, respectively. These peaks are formed owning to the reduction of complex NiOx species

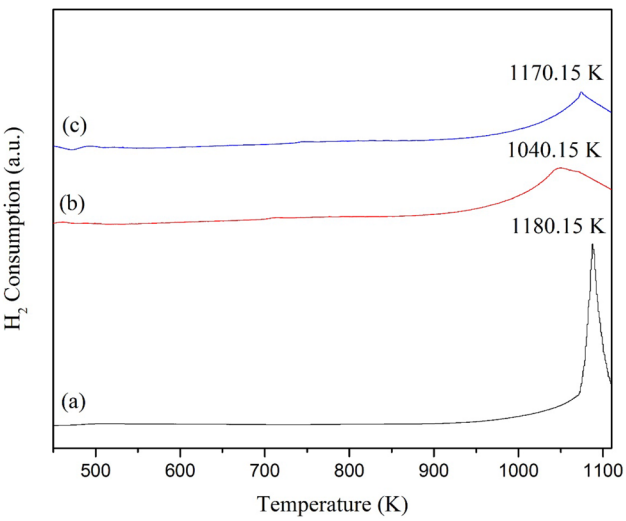

Fig. 4 H_2-TPR patterns of the synthesized catalysts. (a) CAT-1; (b) CAT-2; (c) CAT-3

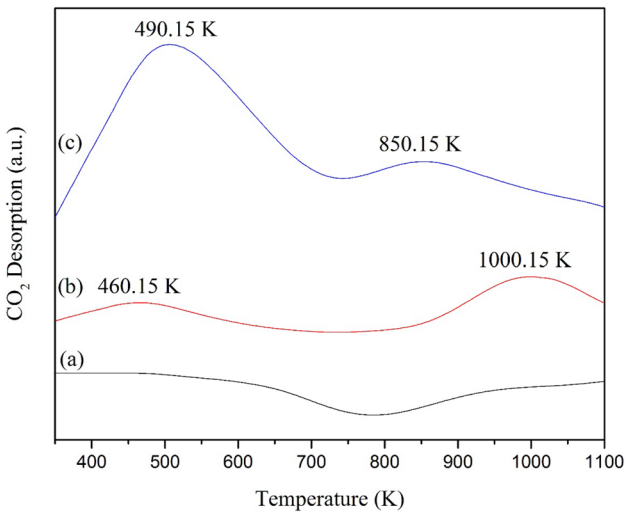

Fig. 5 CO_2-TPD patterns of the synthesized catalysts. (a) CAT-1; (b) CAT-2; (c) CAT-3

which has a strong interaction between the active metals and catalyst support [21].

CO_2-TPD analysis

The CO_2 desorption patterns shown in Fig. 5 display the weak base sites' peak around 490.15 K and the strong base sites' peaks around 850.15 K. In CAT-3, the desorption temperature shifted to the higher location due to the formation of $MgAl_2O_4$ that has strong basic properties. The amount of CO_2 absorbed is increased, and offers more oxygen species on the surface of the catalyst which is useful for the DRM reaction [12]. Hence, an increase in the supports' Lewis basicity could result in a coke-free DRM reaction which boosts the capability of catalysts to chemisorb CO_2, which reacts with C to form CO [12]. Also, this result supports the discussion in XRD analysis implying that the $MgAl_2O_4$ formation posses high resistance to carbon formation and strong metal–surface interaction which could improve the conversion of reactants.

Catalytic performance in DRM

An ideal catalyst for DRM reaction should have two significant properties which are the stability and high activity performance. Figure 6 illustrates the catalytic performances of CAT-1, CAT-2 and CAT-3 in the DRM reaction at 8-h time on stream. Moreover, there is an insignificant occurrence of the reverse water–gas shift (RWGS) reaction on the catalyst which is indicated by the H_2/CO ratio trend that is approximately close to 1, and it is in line with the results found by Zhang et al. [34].

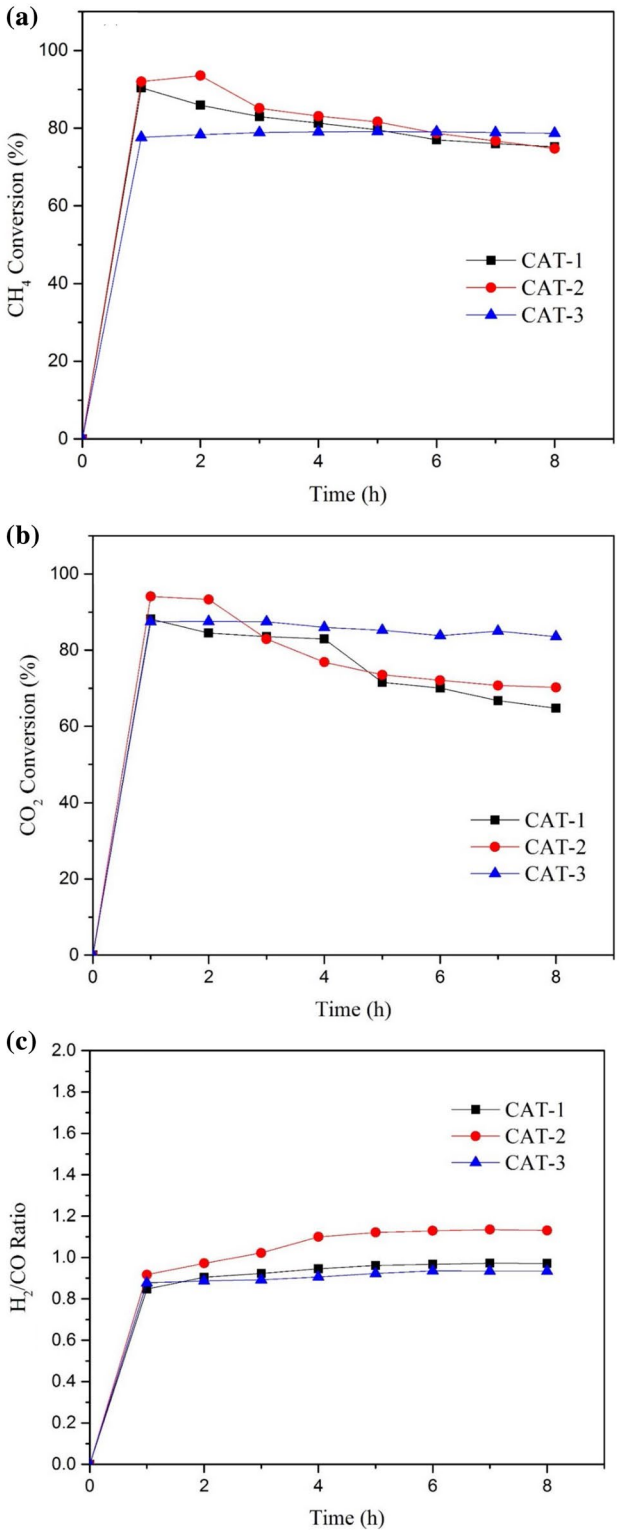

Fig. 6 The catalytic performance of **a** CH_4 conversion; **b** CO_2 conversion; and **c** H_2/CO ratio in DRM presented by synthesized catalysts under the following reaction conditions: $T = 1073.15$ K, $P = 1$ atm, $CH_4 = 20$ mL min^{-1}, $CO_2 = 20$ mL min^{-1}. Symbols represent: (black filled square line) CAT-1, (red filled circle line) CAT-2 and (blue filled triangle line) CAT-3

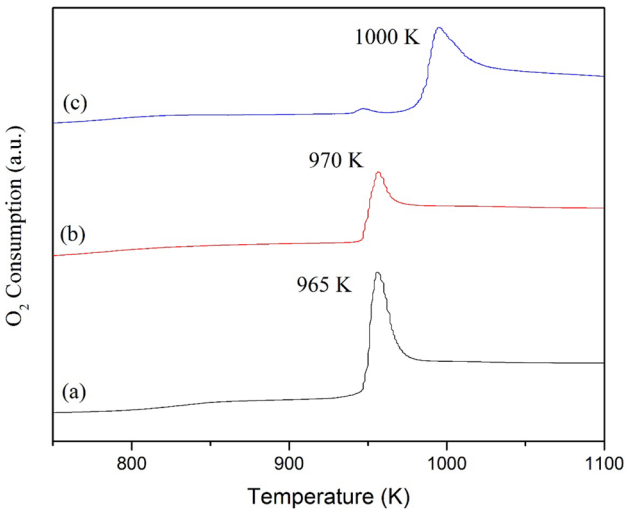

Fig. 7 Temperature programmed oxidation with 5% O_2 in He, performed after 8 h reaction

At the early reaction time, CAT-1 and CAT-2 have higher conversions for both CH_4 and CO_2 compared to CAT-3. However, the conversion of CAT-1 and CAT-2 keep on decreasing, implying that they are unstable throughout the reaction time. On the other hand, CAT-3 is the most stable but less active. This may be due to the low BET surface area of CAT-3 compared to the other two catalysts. However, the basic properties of MgO improve the support interaction and have high stability performance throughout the reaction. Also, the cooperation between Ni and Co results in high performance of catalysts in the DRM reaction. The employment of MgO also produces $MgAl_2O_4$ spinel type that enhances the carbon resistance of the catalyst. The average conversions of CH_4 and CO_2 for CAT-3 are higher, which are 79.17% and 84.82%, respectively, compared to the conversion of CH_4 and CO_2, which were only 55.7% and 60.9%, obtained from the results of Ni/Al_2O_3 catalyst prepared by Min et al. [25] with the reaction temperature of 1073.15 K and pressure of 1 atm.

Post-reaction analysis

TPO was executed to investigate the coke formation in the DRM reaction for the duration of 8 h. The amount of carbon dioxide formed during TPO quantifies the amount of coke formed during the reaction, and the temperature needed to burn off the carbon is an indicator for the carbon bond strength with the catalyst surface. Figure 7 conveys the CO_2 production during TPO in 5% of O_2 in N_2 after DRM reaction. CAT-1 has the highest amount of coke formed, and a temperature of 1000 K is needed to oxidize most of it. The CO_2 evolution at greater than 723 K indicates the oxidation of whisker-type carbon that does not deactivate the nickel surface but slightly causes a breakdown of the catalyst by pore plugging [15].

Conclusion

A comparison between the three synthesized Ni–Co bimetallic catalysts is accomplished. The addition of MgO as the catalyst support into the bimetallic catalyst supported Al_2O_3 decreases the BET surface area and pore volume as MgO has low surface area which causes pore-filling during the catalyst preparation. XRD analysis proves that there is a formation of $MgAl_2O_3$ spinel-type solid solution which has high resistance to coke formation and high metal–support interaction. Hence, CAT-3 that is $Ni–Co/Al_2O_3–MgO$ gives the highest catalyst performance compared to the other synthesized catalysts due to the addition of MgO which enhances the metal–support interaction, and suppresses the carbon formation in DRM reaction that can lead to the high stability and activity performance of the catalysts.

Acknowledgements The authors thankfully acknowledge Universiti Teknologi PETRONAS, Malaysia in providing the necessary facilities to conduct the project.

References

1. Abbasi Z, Haghighi M, Fatehifar E, Rahemi N (2012) Comparative synthesis and physicochemical characterization of CeO_2 nanopowder via redox reaction, precipitation and sol–gel methods used for total oxidation of toluene. Asia Pac J Chem Eng 7(6):868–876
2. Abdollahifar M, Haghighi M, Sharifi M (2016) Sono-synthesis and characterization of bimetallic $Ni–Co/Al_2O_3–MgO$ nanocatalyst: effects of metal content on catalytic properties and activity for hydrogen production via CO_2 reforming of CH_4. Ultrason Sonochem 31:173–183
3. Abdullah B, Abd Ghani NA, Vo D-VN (2017) Recent advances in dry reforming of methane over Ni-based catalyst. J Clean Prod 162:170–185
4. Al-Fatesh ASA, Fakeeha AH (2012) Effects of calcination and activation temperature on dry reforming catalysts. J Saudi Chem Soc 16:55–61
5. Alotaibi R, Alenazey F, Alotaibi F, Wei N, Al-Fatesh A, Fakeeha A (2015) Ni catalysts with different promoters supported on zeolite for dry reforming of methane. Appl Petrochem Res 5(4):329–337
6. Aramouni NAK, Touma JG, Tarboush BA, Zeaiter J, Ahmad MN (2018) Catalyst design for dry reforming of methane: analysis review. Renew Sustain Energy Rev 85(3):2570–2585

7. Asencios Yvan JO, Assaf EM (2013) Combination of dry reforming and partial oxidation of methane on NiO–MgO–ZrO_2 catalyst: effect of nickel content. Fuel Process Technol 106:247–252
8. Ay H, Üner D (2015) Dry reforming of methane over CeO_2 supported Ni, Co and Ni–Co catalysts. Appl Catal B 179:128–138
9. Bradford MCJ, Vannice MA (1999) CO_2 reforming of CH_4. Catal Rev 41(1):1–42
10. Dokamaingam P, Laosiripojana N, Soottitantawat A, Assabumrungrat S (2010) Alternative concept for SOFC with direct internal reforming operation: benefits from inserting catalyst rod. AIChE J 56(6):1639–1650
11. Du X, Zhang D, Shi L, Gao R, Zhang J (2012) Morphology dependence of catalytic properties of Ni/CeO_2 nanostructures for carbon dioxide reforming of methane. J Phys Chem C 116(18):10009–10016
12. Eltegaei H, Reza Bozorgzadeh H, Towfighi J, Reza Omidkhah M, Rezaei M, Zanganeh R, Zamaniyan A, Zarrin Ghalam A (2012) Methane dry reforming on Ni/$Ce_{0.75}Zr_{0.25}O_2$–$MgAl_2O_4$ and Ni/$Ce_{0.75}Zr_{0.25}O_2$–γ-alumina: effects of support composition and water addition. Int J Hydrog Energy 37:4107–4118
13. Fan M-S, Abdullah AZ, Bhatia S (2009) Catalytic technology for carbon dioxide reforming of methane to synthesis gas. Chem Catal Chem 1(2):192–208
14. Fan M-S, Abdullah AZ, Bhatia S (2011) Hydrogen production from carbon dioxide reforming of methane over Ni–Co/MgO–ZrO_2 catalyst: process optimization. Int J Hydrog Energy 36(8):4875–4886
15. Ginsburg JM, Pina J, Solh TE, Lasa HI (2005) Coke formation over a nickel catalyst under methane dry reforming conditions: thermodynamic and kinetic models. Ind Eng Chem Res 44:4846–4854
16. Gonzalez RD, Lopez T, Gomez R (1997) Sol–gel preparation of supported metal catalysts. Catal Today 35(3):293–317
17. Guo J, Lou H, Zhao H, Chai D, Zheng X (2004) Dry reforming of methane over nickel catalysts supported on magnesium aluminate spinels. Appl Catal A 273(1–2):75–82
18. Hassani Rad SJ, Haghighi M, Alizadeh Eslami A, Rahmani F, Rahemi N (2016) Sol–gel vs. impregnation preparation of MgO and CeO_2 doped Ni/Al_2O_3 nanocatalysts used in dry reforming of methane: effect of process conditions, synthesis method and support composition. Int J Hydrog Energy 41(11):5335–5350
19. Iqbal F, Mutalib MIA, Shaharun MS, Khan M, Abdullah B (2016) Synthesis of $ZnFe_2O_4$ using sol–gel method: effect of different calcination parameters. Proc Eng 148:787–794
20. Jiang Z, Liao X, Zhao Y (2013) Comparative study of the dry reforming of methane on fludised aerogel and xeroge; Ni/Al_2O_3 catalysts. Appl Petrochem Res 3(3–4):91–99
21. Koo KY, Roh H-S, Seo YT, Seo DJ, Yoon WL, Bin Park S (2008) A highly effective and stable nano-sized Ni/MgO–Al_2O_3 catalyst for gas to liquids (GTL) process. Int J Hydrog Energy 33:2036–2043
22. Kumar N, Wang Z, Kanitkar S, Spivey JJ (2016) Methane reforming over Ni-based pyrochlore catalyst: deactivation studies for different reactions. Appl Petrochem Res 6(3):201–207
23. Li H, Bok K, Park Y, Yoo J (2011) An efficient mobile peer to peer architecture in wireless Ad Hoc network. In: Lee G, Howard D, Ślęzak D (ed) Convergence and hybrid information technology: 5th international conference, ICHIT 2011, Daejeon, Korea, September 22–24, 2011. Proceedings. Springer, Berlin, pp 1–8
24. Liu D, Quek X-Y, Wah HHA, Zeng G, Li Y, Yang Y (2009) Carbon dioxide reforming of methane over nickel-grafted SBA-15 and MCM-41 catalysts. Catal Today 148(3–4):243–250
25. Min J-E, Lee Y-J, Park H-G, Zhang C, Jun K-W (2015) Carbon dioxide reforming of methane on Ni–MgO–Al_2O_3 catalysts prepared by sol–gel method: effects of Mg/Al ratios. J Ind Eng Chem 26:375–383
26. Papadopoulou C, Matralis H, Verykios X (2012) Utilization of biogas as a renewable carbon source: dry reforming of methane. In: Guczi L, Erdôhelyi A (eds) Catalysis for alternative energy generation. Springer Science + Business Media, New York, pp 57–127
27. Pompeo F, Nichio NN, Souza MMVM, Cesar DV, Ferretti OA, Schmal M (2007) Study of Ni and Pt catalysts supported on α-Al_2O_3 and ZrO_2 applied in methane reforming with CO_2. Appl Catal A 316(2):175–183
28. Rostrupnielsen JR, Hansen JHB (1993) CO_2-reforming of methane over transition metals. J Catal 144(1):38–49
29. Sajjadi SM, Haghighi M, Rahmani F (2014) Dry reforming of greenhouse gases CH_4/CO_2 over MgO-promoted Ni–Co/Al_2O_3–ZrO_2 nanocatalyst: effect of MgO addition via sol-gel method on catalytic properties and hydrogen yield. J Sol Gel Sci Technol 70:111–124
30. Selvarajah K, Phuc NHH, Abdullah B, Alenazey F, Vo D-VN (2015) Syngas Production from methane dry reforming over Ni/Al_2O_3 catalyst. Res Chem Intermed 42(1):269–288
31. Shin SA, Noh YS, Hong GH, Park JI, Song HT, Lee K-Y, Moon DJ (2018) Dry reforming of methane over Ni/ZrO_2–Al_2O_3 catalysts: effect of preparation methods. J Taiwan Inst Chem Eng 90:25–32
32. Xu J, Zhou W, Li Z, Wang J, Ma J (2009) Biogas reforming for hydrogen production over nickel and cobalt bimetallic catalysts. Int J Hydrog Energy 34(16):6646–6654
33. Xu L, Song H, Chou L (2013) Ordered mesoporous MgO–Al_2O_3 composite oxides supported Ni-based catalysts for CO_2 reforming of CH_4: effects of basic modifier and mesopore structure. Int J Hydrog Energy 38(18):7307–7325
34. Zhang X, Zhang Q, Tsubaki N, Tan Y, Han Y (2015) Carbon dioxide reforming of methane over Ni nanoparticles incorporated into mesoporous amorphous ZrO_2 matrix. Fuel 147:243–252
35. Zhang ZL, Tsipouriari VA, Efstathiou AM, Verykios XE (1996) Reforming of methane with carbon dioxide to synthesis gas over supported rhodium catalysts. J Catal 158(1):51–63